ELSEVIER

Colloids and Surfaces
A: Physicochemical and Engineering Aspects 167 (2000) 131–142

COLLOIDS AND SURFACES A

www.elsevier.nl/locate/colsurfa

Ester containing aggregates in the autocatalytic biphasic hydrolysis of ethyl alkanoate

J. Tixier, V. Pimienta, T. Buhse [1], D. Lavabre, R. Nagarajan [2], J.C. Micheau *

Laboratoire des IMRCP, UMR CNRS 5623, Université Paul Sabatier, 118 Route de Narbonne, F-31062 Toulouse Cedex, France

Abstract

Autocatalytic kinetics are observed during the biphasic alkaline hydrolysis of C-4, C-6 and C-8 (butanoate, hexanoate and octanaoate) ethyl esters. Ethanol and alkanoate anions are the products of the reaction. A kinetic model including spontaneous dissolution of the organic phase into the aqueous phase, aqueous hydrolysis of the ester, formation of ester containing aggregates and micellisation has been proposed. For C-4, taking into account salting-in and solvent effects is sufficient to reproduce the autocatalytic behaviour. For C-8, the major autocatalytic process is an ester containing aggregates (ECA) mediated phase transfer. For C-6, it appears that the role of ECA is double. Small sized ECA which are formed at the beginning of the reaction do not perform rapid phase transfer and trap surfactant molecules. Larger ECA which appear at the end of the reaction are the main phase transfer agent. Using an empirical formula to describe the size of the interface, the model is able to reproduce the effect of a variation of the volumic ratio of the two phases as well as the effect of stirring rate and non-emulsified experiments.

Keywords: Autocatalytic biphasic hydrolysis; Ethyl alkanoates; Kinetic model

1. Introduction

In a recent paper, Bachmann et al. [1] reported a reaction in which the formation of micelles apparently occurred autocatalytically. In this reaction ethyl octanoate hydrolyses in biphasic medium to yield ethanol and surfactant ions octanoate, which can aggregate and form micelles. The kinetics of this reaction is characterised by an induction period during which little seems to happen, followed by a sudden increase in the reaction rate. In this second phase the ester is rapidly consumed and a single transparent phase is eventually obtained towards the end of the reaction. Although several models have been proposed to account for such dynamics, its underlying mechanism is still unclear. Moreover, it is puzzling that such autocatalysis is observed since anionic micelles are known to inhibit rather than catalyse bimolecular reactions involving aqueous hydroxide ions.

* Corresponding author. Tel.: +33-561-556-275; fax: +33-561-251-733.

E-mail address: micheau@gdp.ups-tlse.fr (J.C. Micheau)

[1] Present address: Department of Chemistry, Wake Forest University, Winston-Salem, NC 27109, USA.

[2] Permanent address: Department of Chemical Engineering, The Pennsylvania State University, University Park, PA 16802, USA.

0927-7757/00/$ - see front matter
PII: S0927-7757(99)00470-7

In a previous paper [2], we proposed a mechanism to account for the autocatalytic nature of the surfactant formation reported by Bachmann [1]. According to our model, autocatalysis occurs as a result of phase transfer of esters by surfactant molecules formed in the aqueous phase. Numerical simulations using this mechanism showed very good agreement with experimental results on C-8 esters.

In the present paper we extend our work to a wider range of esters, from C-4 to C-8. In order to facilitate the development of a model applicable to this wider range of esters, limiting cases C-4 and C-8 are first considered individually. C-5 to C-7 esters are then treated as intermediate cases. Our model satisfactorily reproduces all of the features observed experimentally, viz. the decrease in total reaction time as the chain length decreases, the observation of autocatalysis in all cases even in the case of short chains such as C-4 — which is quite unexpected since ethyl butanoate (C-4) is known not to form aggregates in the concentration range used in our experiments, and the reaction extent before marked acceleration. It is to be noted that most of our experiments have been carried out under stirred conditions leading to an emulsified medium.

2. Experimental section

2.1. Reagents

Reagents of highest purity commercially available (Fluka) were used without further purification. Alkyl chains are C-4: butanoate, C-6: hexanoate and C-8 octanoate. Sodium hydroxide (pro analysis) was purchased from Prolabo and water was doubly distilled.

2.2. Biphasic hydrolysis of ethyl alkanoates

C-4 and C-8 reactions were performed in a thermostated (T = 80 or 60°C) round-bottom two neck 250 ml flask under reflux. Macro-mixing of the two phases (70 ml aqueous 3M NaOH and 23 ml ester) was achieved by magnetic stirring at 800 ± 5 rpm with an ellipsoidal magnetic bar of $\approx 25 \times 6$ mm size. Initial amounts were: $OH^- = 0.21$ mol and $E_{org} = 0.163$, and 0.116 mol for, respectively, C-4 (60°) and C-8 (80°) experiments. At fixed time intervals the reaction mixture was poured into a graduated volumetric cylinder and after phase separation (within a few seconds) the volume of the residual organic phase was measured. C-6 experiments were performed in a graduated volumetric cylindrical reactor (section was 18.9 cm^2) at T = 80°C using a 2.5×0.5 cm length stirring bar. The initial volume of the aqueous phase was 38.5 ml. The time elapsed during the measurements was accounted for. Non emulsified experiments have been performed in two cylindrical reactors with different cross-sections, viz. 18.9 and 3.3 cm^2, using gentle stirring of the aqueous phase. Due to practical difficulties in maintaining long term stable experimental conditions, the experiment of Fig. 6(b) was stopped after 10 days.

2.3. Model calculations

The general algorithm combines a semi implicit Runge–Kutta method for the numerical integration of the differential equations and a nonlinear minimisation procedure, both of which have been implemented on a HP 9000-710 workstation. Fitting calculations were started using rough estimations of the unknown parameters.

3. Results

3.1. Short chain length esters C-4: the case of ethyl butanoate

Since sodium butanoate is not known to form aggregates in the concentration range used for this experiment (0–1.8 mol l^{-1}), its hydrolysis in an aqueous/oil (biphasic) medium can be represented by the following two-step process:

$$E_{org} \rightleftarrows E_{aq} \qquad r_1 = k_1.Int.\exp(\alpha.(n_{EtOH} + n_S)/V_{aq})$$

$$r_{-1} = k_{-1}.Int.n_{E_{aq}} \qquad \text{(R1)}$$

$$E_{aq} + OH^- \rightarrow S + EtOH \quad r_2 = k_2.n_{E_{aq}}.(n_{OH^-})/V_{aq} \qquad \text{(R2)}$$

where E_{org} and E_{aq} represent, respectively, ethyl butanoate (Ester) in the organic phase and in the water phase, and S the related surfactant. The rates associated with each reaction are expressed to the right of both steps. r_1 represents the rate at which the ester dissolves in the aqueous medium [3]. In this model the rate is taken to be proportional to the 'size' of the interface *Int* (i.e. the droplet total surface area, assuming that the surface of every droplet is composed only of ester molecules; it is therefore proportional to the number of mol of ester on that surface). This rate will also depend on the concentration of both surfactant (salting-in) and ethanol products (solvent effect) [4]. Since, according to Nagarajan [5], the solvent effect is exponentially proportional to the ethanol concentration, we assume a similar dependency on the surfactant concentration, hence the extra term n_S in the exponential function in r_1. The parameter α can therefore be thought of as the solubility enhancement due to ethanol and alkanoate. Here n_x stands for the number of mol of species X, V_{aq} the volume of the aqueous phase, and k_1 the rate constant associated with the overall dissolution process. V_{aq}, is calculated using the conservation relationship $V_{aq} = V_{tot} - V_{org}$ where V_{tot} is the total volume, considered constant, and V_{org} the volume of the organic phase. The latter is calculated at every time step from $V_{org} = V_m.n_{E_{org}}$, where V_m is the molar volume of the ester. Let us note that since solubility is independent of the available quantity of solute, the rate law r_1 is zero order with respect to E_{org}. The rate of the reverse process, r_{-1}, is on the other hand only proportional to the size of the interface *Int* and the number of mol of ester in the aqueous phase E_{aq}. r_{-1} is thus first order with respect to E_{aq}. In our simulations, the ratio k_1/k_{-1} is calculated so that when reaction Eq. (R2) does not take place, saturation ($Solub_0$) is obtained at equilibrium. The amount of ester that can be dissolved in water (with 3 mol l^{-1} salt added) as well as values of α have been evaluated by thermodynamic calculations for the series of esters C-4 to C-8 and are shown in Table 1. Note that according to these calculations, the solubility decreases with increasing chain length.

Step Eq. (R2) represents the hydrolysis of the ester present in the aqueous phase. Its reaction rate is described by a simple bimolecular process, hence our expression of r_2. In previous studies [6,7], rate constants and activation energies have been determined in monophasic binary aqueous solvents with ethanol or acetone as co-solvent. From these studies, it appears that the rate constant for hydrolysis increases with the water contained but is independent of chain length. This allows us to estimate the second order rate constant at the experimental temperature (60°C for ethyl butanoate) to 17 mol^{-1} l per min.

According to the model proposed above, the kinetics associated with the C-4 system can be described by the following set of differential equations:

$$dn_{E_{org}}/dt = -r_1 + r_{-1} \quad (1)$$

$$dn_{E_{aq}}/dt = r_1 - r_{-1} - r_2 \quad (2)$$

$$dn_{OH^-}/dt = -dn_S/dt = -dn_{EtOH}/dt = -r_2 \quad (3)$$

Numerical integration of the above set of equations allows us to calculate the time evolution of the various concentrations. Of particular interest is the volume of the organic phase V_{org}, since this is the quantity measured experimentally. Let us

Table 1
Parameters obtained by thermodynamic calculations[a]

	V_m (l mol^{-1})	$Solub_0$ (mol l^{-1})	α	CMC (mol l^{-1})	g	p_1	g_1	p_2	g_2
C-4	0.132	5.49 10^{-3}	0.56	–	–	–	–	–	–
C-6	0.166	5.30 10^{-4}	0.71	0.3	24	1	2	1	6
C-8	0.199	5.11 10^{-5}	0.85	2.5 10^{-2}	47	–	–	4.5	29

[a] g: average aggregation number for micelles M; p_1: molecules of ester in ECA_1; g_1: average aggregation number for ECA_1; p_2: molecules of ester in ECA_2; g_2: average aggregation number for ECA_2.

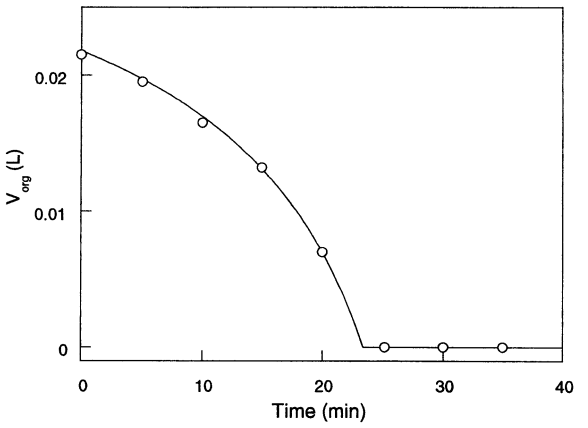

Fig. 1. Volume of the organic phase as a function of time in the biphasic hydrolysis of ethyl butanoate using 3 mol l^{-1} NaOH aqueous solution. T = 60°C, V_{org0}/V_{tot} = 22%, stirring rate: 800 rpm. ○○○: experimental points; —: simulation.

note that in this model the values of k_1 and k_{-1} are initially unknown. However since the dissolution threshold fixes the ratio k_1/k_{-1}($k_1 = k_{-1}.Solub_0$), only one of the two rate constant needs to be determined. Its value is obtained from the best fit to experimental results (parameter optimisation). In the present simulations the value of *Int* is assumed to be constant and equal to one (this will be discussed in more detail later in the paper). Fig. 1 shows the very good agreement between simulations and experimental results.

It should be emphasised that the solubilisation process rate is the rate-determining step in our model. Hydrolysis thus takes place immediately as soon as some ester is present in the aqueous phase. During the course of reaction, our simulations show that the rate of this solubilisation increases by a factor of 8. The cause of this significant increase can be traced back to solvent and salting-in effects, both of which increase exponentially as a function of time according to r_1. This is, according to our model, the origin of the observed autocatalysis.

3.2. Long chain length C-8: the case of ethyl octanoate

The reaction described initially in reference [1] with ethyl octanoate shows a more pronounced non-linear behaviour than the one observed in the case of ethyl butanoate. In particular, the acceleration observed after quite a long induction time, is much stronger than what is observed for ethyl butanoate. As noted in the previous section, the solubility of esters in water decreases with increasing chain length, which results in a smaller contribution to autocatalysis from solvent and salting-in effects. In the case of longer chains such as C-8 the autocatalysis due to solvent and salting-in is not sufficient to account for the acceleration observed in this case. Other processes must therefore be taken into account. We propose that the property of surfactants to form aggregates in the water phase plays a key role for longer chains. A review of the literature [8–11] on this topic leads us to suggest that two types of structures must be considered: mixed aggregates containing ester molecules and micelles formed by surfactants only.

Thermodynamic calculations carried out in non-reactive solution (replacing OH^- by Cl^-) show that small ester-containing aggregates can be formed in the medium at low surfactant concentrations. This is indeed the case at the very beginning of the reaction, before the critical micellar concentration is reached. These so-called 'mixed aggregates' insure phase transfer from the organic to the aqueous phase. These aggregates are then able to transfer and to solubilise ethyl octanoate in the aqueous phase where it is rapidly hydrolysed. This overall process is described by the following scheme:

$$p_2E_{org} + g_2S \rightleftarrows ECA \quad r_3 = k_3.Int.(n_s/V_{aq})^{g_2} \quad r_{-3} = k_{-3}.ECA \qquad (R3)$$

$$ECA \rightleftarrows p_2E_{aq} + g_2S \quad r_4 = k_4.ECA \quad r_{-4} = k_{-4}.E_{aq}.(n_s/V_{aq})^{g_2} \qquad (R4)$$

$$gS \rightleftarrows M \quad r_5 = k_5.S^g.V_{aq}^{1-g} \quad r_{-5} = k_{-5}.M \qquad (R5)$$

where ECA represents ester containing aggregates (mixed aggregates) involving p_2 molecules of ester and g_2 molecules of surfactant. Step Eq. (R3) describes the co-operative aggregation occurring at the interface. A one-step aggregation process is a convenient method for modelling multistep aggregation in this kind of macroscopic kinetic study [12]. The high order rate laws (r_3 and r_{-4})

generate a threshold concentration that can be related to a critical aggregation concentration. The parameter *Int*, the interface size effect, again appears in rate law r_3. The reason for this is that it can be assumed that when a more organic phase is in contact with the water bulk, the aggregation process will be easier, hence the proportionality. As in the previous section *Int* will here be assumed constant for a sake of simplicity. Step R4 describes the phase transfer process: ECA aggregates formed at the interface diffuse to the water bulk, and there, liberate free ester molecules (E_{aq}). Step R5 describes micellisation, as in the case of step R4 it is modelled by a one step high order aggregation where g is the average aggregation number for micelles M. Values for g and the CMC, obtained from thermodynamic calculations, are reported in Table 1. In our simulations, the ratio k_5/k_{-5} is fixed and obtained from Benjamin's calculations [13], viz. $k_5/k_{-5} = CMC^{(1-g)}/2g^2$.

The model for ethyl octanoate hydrolysis involves steps R1 and R2 of Section 3.1 and aggregation processes R3, R4 and R5. The new set of differential equations resulting from simple kinetic equation rules is:

$$dn_{E_{org}}/dt = -r_1 + r_{-1} - p_2(r_3 - r_{-3}) \quad (4)$$

$$dn_{E_{aq}}/dt = r_1 - r_{-1} - r_2 + p_2(r_4 - r_{-4}) \quad (5)$$

$$dn_{OH^-}/dt = -r_2 \quad (6)$$

$$dn_S/dt = r_2 - g_2(r_3 - r_{-3} - r_4 + r_{-4}) - g(r_5 - r_{-5}) \quad (7)$$

$$dn_{EtOH}/dt = r_2 \quad (8)$$

$$dn_{ECA}/dt = r_3 - r_{-3} - r_4 + r_{-4} \quad (9)$$

$$dn_M/dt = r_5 - r_{-5} \quad (10)$$

Numerical integration of the above equations allows us to calculate:

$$V_{org.exp} = V_m(n_{E_{org}} + p_2 n_{ECA}) \quad (11)$$

$V_{org.exp}$ represents experimental values of the volume of the organic phase. Let us note that this volume is different from the volume used for the simulations during the course of reaction. Indeed, to measure the volume of the organic phase during an experiment, stirring is stopped for a while to allow the two phases to separate. We consider that ester molecules involved in ECA are liberated in the organic phase when stirring is stopped. This assumption is based on the fact that no ester is detected in the water phase by Infra Red measurements (as described in [2]). Fig. 2 shows the result of simulations based on the model. As in Section 3.1, the rate of solubilization is optimised through k_{-1}. For mixed aggregation process steps, R3 and R4, both direct and reverse rate constants are obtained by optimisation (see Table 2).

As seen in Fig. 2, our model shows good agreement with the experimental data. After an induction period, during which surfactant molecules accumulate to reach the critical aggregation concentration, phase transfer mediated by ester containing aggregates takes place and a strong acceleration of the reaction is observed. Finally, when all the ester has been consumed, micelles are formed in the medium. One notes that mixed aggregates are formed at an earlier stage than micelles. This is to be expected since the associated rate law is of a lower reaction order than for the micelles (g_2 is 29 for the ECA while the corresponding value of g is 47 for micelles formation (see Table 1)).

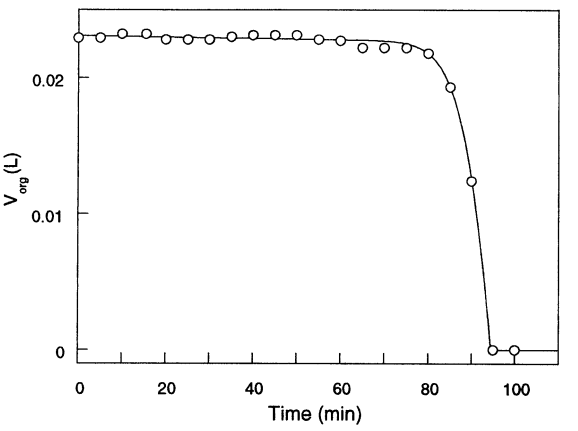

Fig. 2. Volume of the organic phase as a function of time in the biphasic hydrolysis of ethyl octanoate using 3 mol l^{-1} NaOH aqueous solution. T = 80°C, V_{org0}/V_{tot} = 22%, stirring rate: 800 rpm. ○○○: experimental points; —: simulation.

Table 2
Kinetics parameters[a]

	Dissolution		OH^-	ECA_1				ECA_2				M		Interface		
	k_1	k_{-1}	k_2	$k_{3.1}$	$k_{-3.1}$	$k_{4.1}$	$k_{-4.1}$	$k_{3.2}$	$k_{-3.2}$	$k_{4.2}$	$k_{-4.2}$	k_5	k_{-5}	Int_0 (m^2)	*Stir*	β
C-4 and C-8 reactions (Figs. 1 and 2)																
C-4 $_{(60°C)}$	2.82×10^{-3}	5.15×10^{-1}	17	–	–	–	–	–	–	–	–	–	–	*	–	–
C-8	2.57×10^{-7}	5.0×10^{-1}	60	–	–	–	–	2.87×10^{41}	2.3×10^{-2}	1.56	10^{-10}	1.12×10^{57}	1.0×10^{-13}	*	–	–
C-6 non-emulsified reactions (Fig. 6)																
6-(a)	116	2.19×10^{5}	60	2.07×10^{6}	64.3	0.06	9.82	2.26×10^{5}	1.28×10^{3}	13.1	10^{-10}	1.52×10^{-4}	1.6×10^{-13}	1.89×10^{-3}	0	–
6-(b)	"	"	"	"	"	"	"	"	"	"	"	"	"	0.33×10^{-3}	"	–
C-6 emulsified reactions (Fig. 4)																
4-(a, b, c, d)	116	2.19×10^{5}	60	2.07×10^{6}	64.3	0.06	9.82	8.19×10^{7}	9.83×10^{3}	137	10^{-10}	1.52×10^{-4}	1.6×10^{-13}	1.89×10^{-3}	183	128
4-(e)	"	"	"	"	"	"	"	"	"	"	"	"	"	"	497	"
4-(f)	"	"	"	"	"	"	"	"	"	"	"	"	"	"	1013	"

[a] For C-4 and C-8, the parameters in steps R1 and R3 are obtained using $Int = Int_0/s_0 = 1$. For this reason they are not comparable with the ones obtained for C-6. Moreover, the experiments have been carried out in different reactors: C-4 and C-8 in a spherical flask and C-6 in a cylindrical reactor.

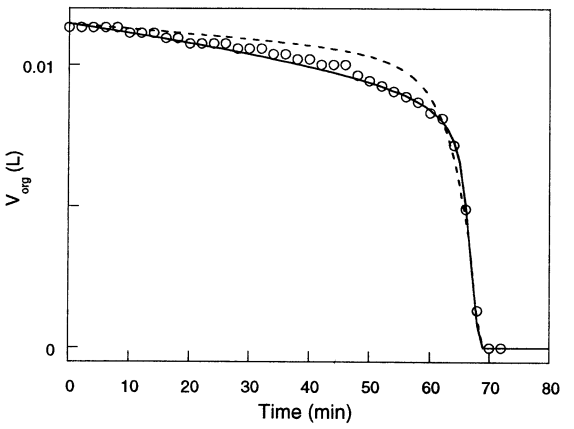

Fig. 3. Kinetics of ethyl hexanoate biphasic hydrolysis. ○○○: experimental points; ----: best fit obtained with the model used in Section 3.2 implying only one size aggregates; —: best fit obtained with the model implying two sizes aggregates.

3.3. Medium chain length C-6: the case of ethyl hexanoate

Our first attempts to fit ethyl hexanoate experimental curves to the model presented in Section 3.2 were met with various difficulties. The kinetics, in this case is characterised by a significant initial slope and by a large reaction extent ($\approx 30\%$ of ester is consumed) before any marked acceleration starts. These properties cannot be reproduced with the model proposed above. More specifically, if we try to reproduce the initial slope then the overall reaction time is found to be too short, phase transfer then taking place too early in the reaction. Alternatively, if one attempts to adjust the parameters to obtain the correct overall reaction then the initial rate becomes too small (Fig. 3). The model proposed for ethyl octanoate is therefore clearly not sufficient to describe medium chain length (C-5 to C-7) kinetics.

In a first attempt to account for this phenomenon we have recently invoked the possibility of surfactant adsorption at the interface during the first stages of reaction [5]. The interface in this case, plays the role of a reservoir where surfactant molecules are temporarily stored, and therefore unavailable for the phase transfer process.

To gain further insight into this phenomenon, several experiments were carried out. One of the key results is that in experiments with fixed interface size (without emulsification), only the reaction time and not the extent of reaction before acceleration is affected by size of the interface. In these experiments the reaction is carried out without emulsifying the mixture. Only the bulk of the water phase is slowly stirred for homogenisation. In order to see the effect of the size of the interface, two experiments were carried out in cylindrical reactors with different cross-section (see Section 4.1, Fig. 6). If surfactants are indeed stored at the interface at the beginning of the reaction, one would expect that changing the size of the interface would have an effect on the extent of the reaction before any acceleration is observed. In fact, changing the cross-section of the reactor was found to have an effect on the reaction time, the latter being larger for the smaller interface. However, no effect was observed on the extent of the reaction before the start of the acceleration. From these experiments we conclude that the size of the interface indeed has an effect on the overall reaction time but not on the 'storage' process.

Four experiments were carried out with decreasing initial volumes of ester, viz. from 11.5 ml (0.069 mol) to 3 ml (0.018 mol). Since the 30% extent corresponds to 0.021 mol of ester consumed, one would expect that no significant acceleration is observed for those experiments in which the initial number of mol of ester is smaller than this value. As shown in Fig. 4, this is indeed what is observed experimentally: the first three experiments (Fig. 4(a), (b) and (c)) show a marked acceleration while the last one (Fig. 4(d)), involving less than 0.021 mol of ester does not. However, the three experiments, with higher organic volume, present the same extent before acceleration (30%).

Before presenting the model for the case of C-6 esters let us briefly discuss the effect of the initial organic volume on the reaction time. It is observed experimentally that the overall reaction time increases as the initial volume of the organic phase decreases. It is suggested that this phenomenon is related to the dependence of reaction

time on the size of the interface. Assuming that when the stirring rate is maintained constant, the size of the droplets formed by emulsification remains the same, decreasing the organic volume thus decreases the number of ester droplets, hence the interface size and therefore the overall reaction time.

Finally we have carried out two more experiments using faster stirring rates (Fig. 4(a), (e) and (f)). The kinetics curves obtained support the above interpretation.

The purpose of what follows is to propose a model that can account for the results discussed above, namely (i) the large reaction extent before acceleration, and (ii) the effect of the size of the interface on the overall reaction time. In the mechanism proposed for ethyl octanoate reaction, mixed aggregates responsible for phase transfer are assumed to be monodispersed. In fact, thermodynamic calculations show that the formation of aggregates should start at the very beginning of the reaction, which implies that the size of these aggregates should increase as a function of time. Moreover, these calculations also show that in smaller aggregates, ester molecules have a greater tendency to be located in the core of the structure, while in the case of larger ones they locate themselves closer to the periphery (between surfactants tails). The ratio between ester molecules in the core and at the periphery decreases as the structures grow. As a result, smaller aggregates are not expected to dissociate as easily as larger ones in the water phase, therefore inhibiting phase transfer in the early stage of the reaction. Larger aggregates are then solely responsible for the phase transfer process. In order to account for the different properties of small and large aggregates steps (R3 and R4) from the preceding model are duplicated.

$$p_1.E_{org} + g_1.S \rightleftarrows ECA_1 \quad r_{3.1} = k_{3.1}.Int.(n_s/V_{aq})^{g_1}$$
$$r_{-3.1} = k_{-3.1}.n_{ECA_1} \qquad \text{(R3.1)}$$

$$ECA \rightleftarrows {}_1p_1.E_{aq} + g_1.S \quad r_{4.1} = k_{4.1}.n_{ECA_1}$$
$$r_{-4.1} = k_{-4.1}.E_{aq}.(n_s/V_{aq})^{g_1} \qquad \text{(R4.1)}$$

$$p_2.E_{org} + g_2.S \rightleftarrows ECA_2 \quad r_{3.2} = k_{3.2}.Int.(n_s/V_{aq})^{g_2}$$
$$r_{-3.2} = k_{-3.2}.n_{ECA_2} \qquad \text{(R3.2)}$$

$$ECA_2 \rightleftarrows p_2.E_{aq} + g_2.S \quad r_{4.2} = k_{4.2}.n_{ECA_2}$$
$$r_{-4.2} = k_{-4.2}.E_{aq}.(n_s/V_{aq})^{g_2} \qquad \text{(R4.2)}$$

where ECA_1 and EAC_2 represent, respectively, smaller and larger ester containing aggregates. The values for p_1, g_1, p_2 and g_2 are estimated from thermodynamic calculations. These calculations show a continuous variation of the aggregates size

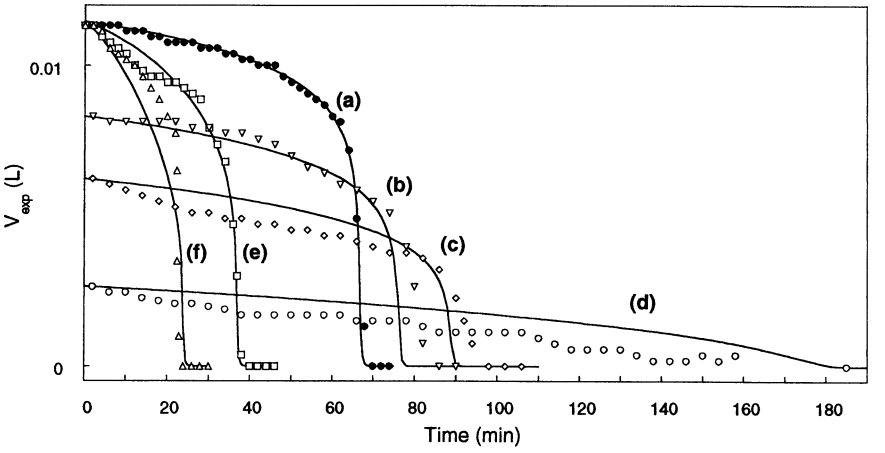

Fig. 4. Kinetics of ethyl hexanoate biphasic hydrolysis. A: effect of initial ester volumes: (a) $V_{org0} = 11.5$ ml (0.069 mol); (b) $V_{org0} = 8.5$ ml (0.051 mol); (c) $V_{org0} = 6.5$ ml (0.039 mol); (d) $V_{org0} = 3$ ml (0.018 mol). Stirring rate is 600 rpm in each case. B: effect of stirring rate: (a) 600 rpm (this experiment is common to both series); (e) 800 rpm; (f) 1050 rpm ($V_{aq0} = 38.5$ ml for all the experiments. —: simulations.)

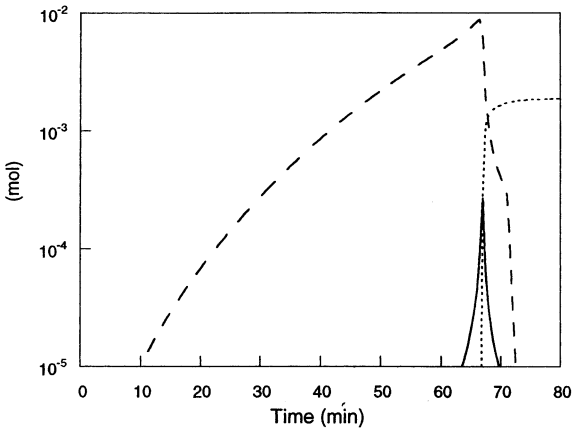

Fig. 5. Concentration profiles obtained from simulation of experimental curve represented in Fig. 3. Dashed line: ECA_1; solid line: ECA_2; dotted line: M.

as a function of the surfactant concentration. Considering that during the reaction course surfactant concentration varies from 0 to 1.38 mol l^{-1}, we have chosen: $p_1 = 1$ and $g_1 = 2$ for the smaller aggregates; this corresponds to a surfactant concentration of 0.01 mol l^{-1}; $p_2 = 1$ and $g_2 = 6$ correspond to a surfactant concentration of 1.3 mol l^{-1}. In this interval, the ratio between ester molecules located in the core and between surfactant tails varies from 5 to 3.

The model used for the simulation of C-6 esters is therefore composed of step R1 and R2 (Section 3.1), steps $R3_1$, $R4_1$, $R3_2$ and $R4_2$ and micellisation step R5 (Section 3.2). The entire model and corresponding set of differential equations are given in Appendix A.

As seen in Fig. 3 the agreement between the model and experimental data is quite good. Duplicating the mixed aggregation process therefore seems sufficient to account for the observed extent of the reaction before acceleration. The smaller aggregates ECA_1, are formed early in the reaction, as soon as the surfactant is produced by the hydrolysis. The parameters obtained from the best fit are such that ECA_1 accumulation is favoured (see Table 2). Larger aggregates ECA_2, are formed later and do not accumulate in such proportion. This favours the liberation of free ester molecules in the aqueous phase, giving rise to phase transfer and strong acceleration. In the final stage of the reaction, micelles are formed. Concentration profiles for the three types of aggregates are given in Fig. 5.

4. Discussion

In order to test the validity of the model presented in this section an attempt has been made to use it to model the results obtained in the case of both non-emulsified and emulsified experiments. Since the emulsification process affects the size of the interface, the parameter *Int* needs to be considered in more detail.

4.1. Non-emulsified experiments

The easiest way to measure the size of the interface is not to emulsify the solution. In this case, the cross section of a cylindrical reactor gives the size of the interface. As mentioned above two reactors have been used, a larger and a smaller one. In a first experiment in the larger reactor the value of $Int = Int_0/s_0$ is used in the simulations. Int_0 is the reactor cross section and s_0 the molar surface of ethyl hexanoate (6×10^4 m^2 mol^{-1}). The best fit to the model then provides us with a set of system parameters which are then used in the case of the smaller reactor. Changing only the value of Int_0 yields a good prediction in the case of the smaller reactor (see Fig. 6 and Table 2 for the best fit parameters).

4.2. Emulsified experiments

The results of the simulations in the case of non-emulsified experiments seem to support the assumption that the parameter *Int* appears correctly in the rate laws. In the case of reactions in an emulsified medium we need to take into account the volume of the organic phase and the effect of the stirring on the emulsification process.

A detailed study of these effects on the size of the interface is beyond the scope of the present paper. Rather, we suggest the following function to take into account the various parameters of interest.

$$Int = (Int_0/s_0)(1 + Stir(V_{org}V_{aq}/V_{tot}^2)(1 + \beta(n_S/V_{aq})) \quad (12)$$

Note that in order for *Int* to become zero at the end of the reaction, $Int = E_{org}$ when $E_{org} < Int$.

Int_0 is the initial interface size before stirring in m^2; it is divided by s_0 the ester molar surface so that *Int* is expressed as a number of mol. We have also arbitrarily decided to use a linear dependency on the following parameters:

Stir, the emulsification efficiency. This parameter is related to the speed of rotation of the magnetic stirrer. For non-emulsified reactions, $Stir = 0$ and $Int = Int_0/s_0$.

$(V_{org}V_{aq}/V_{tot}^2)$: this term accounts for the dependency of the interface area on both organic and aqueous volume. In this very simple expression the size of the interface becomes zero when V_{org} or $V_{aq} = 0$ and goes through a maximum when $V_{org} = V_{aq}$. In the present study, V_{org} decreases and is always smaller than V_{aq}, leading to the decrease of the value of the function as time increases.

$1 + \beta(n_S/V_{aq})$: β accounts for the effect of the surfactant on the interfacial tension. Note that this term results in an increase of the size of the interface during reaction.

Parameter optimisation has been carried out on the experiment corresponding to curve (a) in Fig. 4, which is common to the two emulsified series. Fitting results are represented in the same figure with continuous line, and the parameters obtained are given in Table 2.

Before we test further the interface size function, the first thing we must do is to compare parameters obtained for emulsified solutions with those of the non-emulsified ones. For the emulsified reactions the formation of ECA_2 is faster (see $k_{3.2}$, $k_{-3.2}$, Table 2); this could be related to easier aggregate formation caused by intense stirring [14]. The rate constant ($k_{4.2}$) corresponding to the liberation of E_{aq} in the water phase is also increased favouring phase transfer for emulsified solutions.

In the case of experiments involving different initial volumes of ester, predicted results (Fig. 4) reproduce qualitatively the main properties: reaction time increases, and the loss of strong acceleration for the experiment involving less ester. The discrepancies observed between simulation and experiments are not surprising taking into account the simple function used to model the size of the interface. Concerning experiments for which an increased stirring rate has been used, the experimental reaction time is obtained varying the corresponding parameter *Stir* (see Table 2). Better fitting results can be obtained just by increasing $k_{4.2}$, corresponding to the ECA_2 formation (not shown).

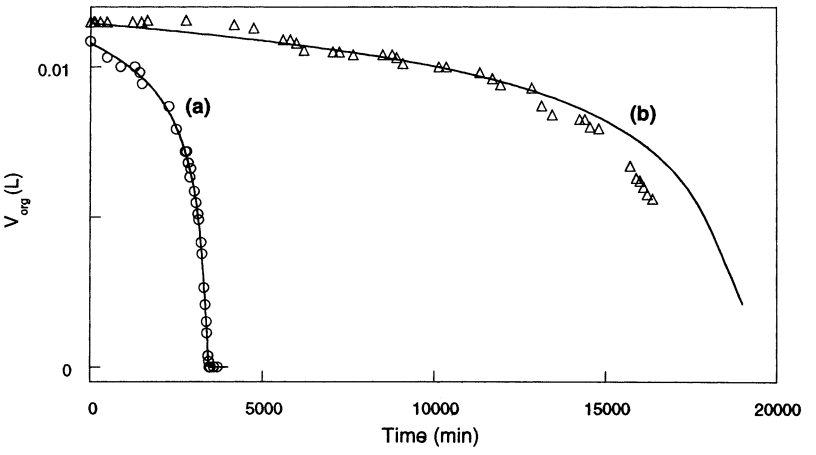

Fig. 6. Non-emulsified reaction: (a) cross section surface is 18.9 cm^2 (fitted); (b) cross section surface is 3.3 cm^2 (predicted using parameters obtained for curve (a). ○○○: experience, —: simulation.

5. Conclusions

In this paper, the origin for autocatalytic behaviour in biphasic ethyl alkanoates is discussed. Mechanisms proposed are tested using kinetic modelling and inverse treatment. This allows us to propose the simplest models capable of reproducing experimental curves, and still providing comprehensive information on mechanisms. The last model proposed accounts for the whole chain length series. This model takes into account all the processes needed to interpret the different behaviours: solubility enhancement caused by product formation in the case of ethyl butanoate, phase transfer mediated by ester containing aggregates for ethyl octanoate. In the case of ethyl hexanoate two size aggregates need to be invoked to explain phase transfer inhibition in the beginning of the reaction. Using the same model and the corresponding thermodynamic parameters ethyl pentanoate and heptanoate hydrolysis can be correctly fitted. The interface size effect although translated by a rather simple function accounts for initial organic volume and stirring rate variations.

Acknowledgements

We thank Dr J.P. Laplante for rereading the manuscript.

Appendix A. Equations for the complete model

$$E_{org} \rightleftarrows E_{aq} \quad r_1 = k_1.Int.\exp(\alpha(n_{EtOH} + n_S)/V_{aq})$$
$$r_{-1} = k_{-1}.Int.n_{E_{aq}} \quad \text{(AR1)}$$

$$E_{aq} + OH^- \rightarrow S + EtOH \quad r_2 = k_2.n_{E_{aq}}(n_{OH^-})/V_{aq} \quad \text{(AR2)}$$

$$p_1.E_{org} + g_1.S \rightleftarrows ECA_1 \quad r_{3.1} = k_{3.1}.Int.(n_s/V_{aq})^{g_1}$$
$$r_{-3.1} = k_{-3.1}.n_{ECA_1} \quad \text{(AR3.1)}$$

$$ECA_1 \rightleftarrows p_1.E_{aq} + g_1.S \quad r_{4.1} = k_{4.1}.n_{ECA_1}$$
$$r_{-4.1} = k_{-4.1}.E_{aq}(n_s/V_{aq})^{g_1} \quad \text{(AR4.1)}$$

$$p_2.E_{org} + g_2.S \rightleftarrows ECA_2 \quad r_{3.2} = k_{3.2}.Int.(n_s/V_{aq})^{g_2}$$
$$r_{-3.2} = k_{-3.2}.n_{ECA_2} \quad \text{(AR3.2)}$$

$$ECA_2 \rightleftarrows p_2.E_{aq} + g_2.S \quad r_{4.2} = k_{4.2}.n_{ECA_2}$$
$$r_{-4.2} = k_{-4.2}.E_{aq}.(n_s/V_{aq})^{g_2} \quad \text{(AR4.2)}$$

$$g.S \rightleftarrows M \quad r_5 = k_5.n_S^g.V_{aq}^{1-g} \quad r_{-5} = k_{-5}.n_M \quad \text{(AR5)}$$

Where:

r_j are in mol min^{-1}, assuming rate constants k_j in usual units;

$$Int = (Int_0/s_0) \times (1 + Stir(V_{org}.V_{aq}/V_{tot}^2)(1 + \beta(n_S/V_{aq}))$$

(if $E_{org} < Int$ then $Int = E_{org}$)

$V_{org} = V_m.n_{E_{org}}$ ($V_m = E_{org}$ molar volume)

$V_{aq} = V_{tot} - V_{org}$ (assuming V_{tot} constant)

$k_1 = k_{-1}.Solub_0$;

$k_5 = k_{-5}.CMC^{1-g}/g^2$

List of variables

n_x	The number of mol of species X
E_{org}	Ethyl alkanoate in the organic phase
E_{aq}	Ethyl alkanoate in the aqueous phase
OH^-	Hydroxide ion
S	Free alkanoate ion
EtOH	Ethanol
ECA_1	Smaller ester containing aggregate
ECA_2	Larger ester containing aggregate
M	Micelles

Experimental data

V_{org}	Volume of the organic phase
V_{aq}	Volume of the aqueous phase
V_{tot}	Total volume
Stir	Rate of stirring
Int_0	Reactor cross section

Thermodynamic parameters

s_0	Molecular area of ethyl alkanoate
V_m	Molecular volume of ethyl alkanoate
$Solub_0$	Saturation solubility of ethyl alkanoate in aqueous phase
α	Correction factor related to salting-in and solvent effect
β	Interfacial tension correction factor
g	Average micellar aggregation number
g_i	Average aggregation number of ECA_i
p_i	Average number of molecules of ester in ECA_i

Differential equations

$$dn_{E_{org}}/dt = -r_1 + r_{-1} - p_1(r_{3.1} - r_{-3.1}) - p_2(r_{3.2} - r_{-3.2})$$

$$dn_{E_{aq}}/dt = r_1 - r_{-1} - r_2 + p_1(r_{4.1} - r_{-4.1}) + p_2(r_{4.2} - r_{-4.2})$$

$$dn_{OH^-}/dt = -r_2$$

$$dn_S/dt = r_2 - g_1(r_{3.1} - r_{-3.1} - r_{4.1} + r_{-4.1}) - g_2(r_{3.2} - r_{-3.2} - r_{4.2} + r_{-4.2}) - g(r_5 - r_{-5})$$

$$dn_{EtOH}/dt = r_2$$

$$dn_{ECA_1}/dt = r_{3.1} - r_{-3.1} - r_{4.1} + r_{-4.1}$$

$$dn_{ECA_2}/dt = r_{3.2} - r_{-3.2} - r_{4.2} + r_{-4.2}$$

$$dn_M/dt = r_5 - r_{-5}$$

Due to the interruption of stirring for measuring, residual organic volume $V_{org.exp}$ is calculated as following:

$V_{org.exp} = V_{org} + V_m(p_1.n_{ECA_1} + p_2.n_{ECA_2})$ if $Stir = 0$ then $V_{org.exp} = V_{org}$

References

[1] P.A. Bachmann, P.L. Luisi, J. Lang, Nature 357 (1992) 57–59.
[2] T. Buhse, R. Nagarajan, D. Lavabre, J.C. Micheau, J. Phys. Chem. A 101 (1997) 3910–3917.
[3] M.H. Abraham, J. Chem. Soc. Faraday Trans. 1 (80) (1984) 153–181.
[4] A.T. Gros, R.O. Feuge, J. Amer. Oil Chem. Soc. August (1952) 313–317.
[5] T. Buhse, D. Lavabre, R. Nagarajan, J.C. Micheau, J. Phys. Chem. A 102 (1998) 10552–10559.
[6] D.P. Evans, J.J. Gordon, H.B. Watson, J. Chem. Soc. (1938) 1439–1444.
[7] G. Davies, D.P. Evans, J. Chem. Soc. (1940) 339–345.
[8] S. Karaborni, N.M. van Os, K. Esselink, P.A.J. Hilbers, Langmuir 9 (1993) 1175–1178.
[9] B. Smit, P.A.J. Hilbers, K. Esselink, L.A.M. Rupert, N.M. van Os, A.G. Schlijper, J.Phys. Chem. 95 (1991) 6361–6368.
[10] B. Smit, P.A.J. Hilbers, K. Esselink, L.A.M. Rupert, N.M. van Os, A.G. Schlijper, Nature 348 (1990) 624–625.
[11] J. Weiss, J.N. Coupland, D.J. McClements, J. Phys. Chem. 100 (1996) 1066–1071.
[12] J.A.D. Wattis, P.V. Coveney, J. Chem. Phys. 106 (22) (1997) 9122–9140.
[13] L. Benjamin, J. Phys. Chem. 68 (12) (1964) 3575–3581.
[14] S.Q. Wang, J. Phys. Chem. 94 (1990) 8381–8384.